

# Invariant properties and rotation transformations of the GPR scattering matrix



Almendra Villela\*, José M. Romo

División de Ciencias de la Tierra, Centro de Investigación Científica y de Educación Superior de Ensenada, Carretera Ensenada-Tijuana #3918, zona Playitas, Ensenada, Baja California 22860, Mexico

## ARTICLE INFO

### Article history:

Received 13 July 2012

Accepted 1 January 2013

Available online 11 January 2013

### Keywords:

GPR scattering matrix

Multiple polarizations

Invariant properties

GPR matrix transformation

## ABSTRACT

We analyze the properties of the scattering matrix associated with the incident and scattered electric fields used in GPR. The elements of the scattering matrix provide information produced by different polarizations of the incident wave field. Rotationally invariant quantities such as trace, determinant and Frobenius norm lead to images that combine the information contained in the four elements of the scattering matrix in a mathematically simple and sound manner. The invariant quantities remove the directional properties implicit in the dipolar field used in GPR allowing the application of standard processing techniques designed for scalar fields, such as those used in seismic data processing. We illustrate the non-directional properties of the invariants using a 3D simulation of the wavefield produced by a point scatterer. The estimation of the azimuth angle of elongated targets is also explored using rotation transformations that maximize alternatively the co-polarized or the cross-polarized responses. The angle estimation is essentially an unstable process, particularly if low amplitudes or noisy data are involved. We apply the Frobenius norm  $\|S\|_F$  as a criterion for selection of the best amplitudes to use for a more stable and significant angle estimation. The performance of our formulation was tested with synthetic data produced by a 3D model of an air-filled metal pipe buried in a homogeneous halfspace. The images resulting from the invariants show a clear diffraction hyperbola suitable for a scalar wavefield migration, while the azimuth of the pipe is neatly resolved for amplitudes selected with  $\|S\|_F \geq 0.4$ . A field experiment conducted above an aqueduct pipe illustrates the proposed methods with real data. The images obtained from the invariants are better than those from the individual elements of the scattering matrix. The azimuth estimated using our formulation is in agreement with the probable orientation of the aqueduct. Finally, a field experiment above a buried air-filled barrel shows that combining the information in the way proposed in this work may lead to an improved image of the subsurface target, the cost to pay is the lost of directional information contained in the scattering matrix. In general, we claim that the methods proposed in this work can be useful to analyze the information acquired by multicomponent GPR surveys using standard scalar wavefield algorithms.

© 2013 Elsevier B.V. All rights reserved.

## 1. Introduction

The vector nature of the electromagnetic fields generated and measured by ground penetrating radars (GPR) prompts the study of the response of buried targets to different field polarizations (Roberts, 1994; Roberts and Daniels, 1996). A number of experiments have been attempted to exploit the use of multicomponent measurements for different subsurface targets. It has been shown that using different polarizations can help to better define the size, shape and orientation of the target. For example, Guy et al. (1999) found that non-planar or rough objects are better imaged using a receiver antenna perpendicular to the polarization of the source (cross-polarization); Radzevicius and Daniels (2000) studied the backscattered fields from cylinders with different polarization properties; they found that high impedance

dielectric pipes are best imaged with the long axis of the dipoles oriented orthogonal to the long axis of the pipes, while using antennas oriented parallel to the long axis of the pipes produces better images for low impedance metallic pipes. In recent years, a number of migration algorithms have been proposed to properly account for the vector nature of GPR wave propagation as well as for dipolar antenna radiation patterns and coupling factors (Lambot et al., 2004; Streich et al., 2007; van der Kruk et al., 2003). Orlando and Slob (2009), using 2.0 GHz multicomponent data to detect cracks in a historical building, found that vector migration images have better resolution than images obtained with standard 2D scalar migration.

On the other hand, it is common that algorithms designed for elastic waves processing (seismic reflection data) be used for GPR data processing. Lehmann et al. (2000) pointed out the convenience of using the sum of copolarized fields to obtain non-directional wavefields suitable for processing with standard scalar wavefield algorithms.

In this work we explore the rotation-invariant properties of the scattering matrix and their ability to transform the characteristic directional

\* Corresponding author at: CICESE/Earth Sciences, P.O. Box 434843, San Diego, CA, 92143-4843, United States. Tel.: +52 646 175 0500; fax: +52 646 175 0567.

E-mail addresses: [avillela@cicese.mx](mailto:avillela@cicese.mx) (A. Villela), [jromo@cicese.mx](mailto:jromo@cicese.mx) (J.M. Romo).

wavefield implicit in GPR measurements to a non-directional field more appropriate for processes designed for scalar wave fields like seismic waves. We also propose an improved way to estimate the orientation of elongated objects by using particular rotation transformations of the scattering matrix.

## 2. The scattering matrix

In a common bistatic GPR system, the transmitting dipolar antenna produces a nearly linearly polarized electromagnetic field oriented mainly parallel to the axis of the antenna. A separate receiver antenna detects the signal backscattered by the targets in the subsurface. The amplitude, polarization, and arrival time of the backscattered field strongly depend on the electromagnetic (EM) properties and geometry of the target, as well as on the subsurface properties. Elongated targets such as pipes or dipping fractures change the polarization of the transmitted wave producing backscattered fields in directions distinct from the transmitting antenna axis. This fact encourages the idea of illuminating the targets and measuring the backscattered field with different antenna orientations in order to obtain information about each target's orientation as well as about its EM properties. Four antenna arrays might be devised to illuminate a target and register the scattered wave field along a profile: two co-polarized arrays and two cross-polarized arrays. In the co-polarized (co-pol) arrays the receiver and transmitter antennas are parallel to each other, while in the cross-polarized (x-pol) mode they are perpendicular. The common practice in GPR profiling is to operate a co-pol array in a "broadside" mode, i.e. with both antennas perpendicular to the profile's direction. Other possibility is setting the co-pol array with both antennas parallel to the profile's direction. For the x-pol array there are also two possible operation modes: one of them with the transmitter perpendicular to the profile's direction and the other parallel to it.

The response of these four arrays is represented by the time-domain scattering matrix  $\mathbf{S}(t)$  (Chen et al., 2001; Sassen and Everett, 2009)

$$\mathbf{S}(t) = \begin{pmatrix} S_{xx} & S_{xy} \\ S_{yx} & S_{yy} \end{pmatrix}, \quad (1)$$

where the first subscript in the elements of the matrix represents the transmitter direction and the second subscript corresponds with the receiver orientation. Thus, co-pol responses are in the diagonal and the off-diagonal elements are x-pol responses. Because of the reciprocity principle, both x-pol arrays are exactly equivalent; however, it is meaningful to acquire field data with both of them as to reduce noise and contribute to the image improvement.

For horizontal planar scatterers both co-pol arrays are identical ( $S_{xx} = S_{yy}$ ) and the x-pol response vanishes ( $S_{xy} = S_{yx} = 0$ ). In contrast, for elongated targets the co-pol responses differ, and the x-pol responses are not null, with their relative amplitude depending on the geometry and electrical properties of the target (Radzevicius and Daniels, 2000). The time-domain matrix  $\mathbf{S}$  is a real-valued symmetric matrix with  $S_{xy} = S_{yx}$  because of the reciprocity principle. Each element in  $\mathbf{S}$  might represent the time-varying radargram in a given location of the Tx-Rx (transmitter-receiver) array, or a whole common-offset section along a given profile.

Applying a simple linear transformation to the scattering matrix, the orientation of the measurement frame can be rotated at different azimuths in order to investigate the target's response as a function of the polarization direction. The scattering matrix in a rotated system is given by

$$\mathbf{S}' = \mathbf{R}\mathbf{S}\mathbf{R}^T, \quad (2)$$

where

$$\mathbf{R} = \begin{pmatrix} \cos\theta & \sin\theta \\ -\sin\theta & \cos\theta \end{pmatrix}, \quad (3)$$

and  $\theta$  is the counterclockwise rotation angle. The elements of the rotated matrix  $\mathbf{S}'$ , in terms of original elements and the rotation angle, are given by

$$\begin{aligned} S'_{xx} &= S_{xx} \cos^2\theta + S_{yy} \sin^2\theta + (S_{yx} + S_{xy}) \sin\theta \cos\theta \\ S'_{xy} &= S_{xy} \cos^2\theta - S_{yx} \sin^2\theta + (S_{yy} - S_{xx}) \sin\theta \cos\theta \\ S'_{yx} &= S_{yx} \cos^2\theta - S_{xy} \sin^2\theta + (S_{yy} - S_{xx}) \sin\theta \cos\theta \\ S'_{yy} &= S_{yy} \cos^2\theta + S_{xx} \sin^2\theta - (S_{yx} + S_{xy}) \sin\theta \cos\theta \end{aligned} \quad (4)$$

For a fixed time, one can plot the four elements of the scattering matrix as a function of the rotation angle, using a polar diagram representation.

Fig. 1a shows the radargrams registered by co-pol and x-pol antenna configurations in a given site. Both co-pol signals,  $S_{xx}$  and  $S_{yy}$ , are very similar in amplitude and shape; the x-pol signals  $S_{xy}$  and  $S_{yx}$  exhibit some differences probably because of measurement inaccuracies and/or noise contamination. Fig. 1b shows polar diagrams obtained at  $t = 19.2$  ns and  $t = 35.2$  ns using the four radargrams in Fig. 1a. The diagrams show the amplitude's absolute value of the four elements of  $\mathbf{S}'$  in the azimuth range  $0^\circ < \theta < 360^\circ$ .

Several properties of the scattering matrix are evident in the polar diagram plot. The co-pol amplitudes are related by  $S'_{xx}(\theta) = S'_{yy}(\theta + 90^\circ)$ , while the x-pol amplitudes, which should be identical because of the reciprocity principle, have some differences attributable to measurement inaccuracy. A remarkable property is that the azimuth that makes  $S'_{xx}$

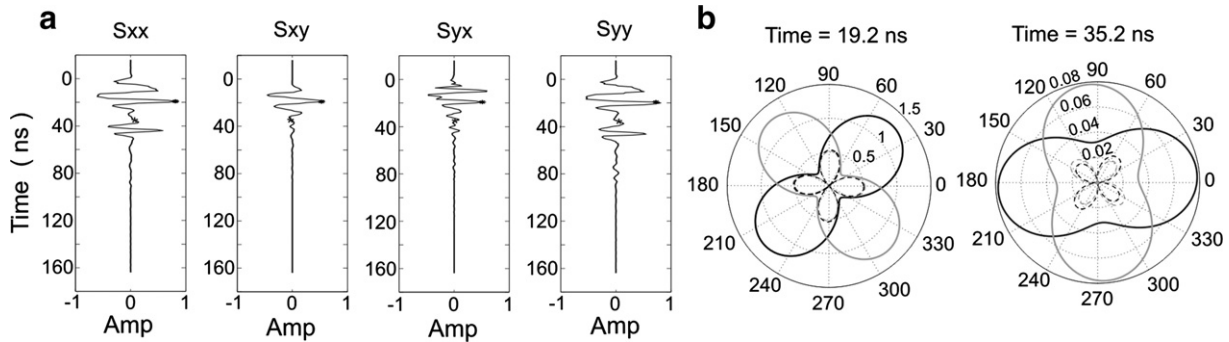


**Fig. 1.** (a) Radargrams showing the four sets of measurements used to fill the elements for the scattering matrix as a function of time. In the radargram, the symbol at  $t = 19.2$  ns and  $t = 35.2$  ns indicates the time selected to calculate the polar diagrams shown in b. The amplitude of the components was normalized only for plotting purposes. (b) Polar diagrams calculated for  $t = 19.2$  ns and  $t = 35.2$  ns. The magnitude of  $S_{xx}(\theta)$  and  $S_{yy}(\theta)$  is shown as continuous black and gray lines, respectively, while the x-pol elements  $S_{xy}(\theta)$  and  $S_{yx}(\theta)$  are the black and gray dashed lines, respectively. Magnitude normalized for plotting purposes.

Download English Version:

<https://daneshyari.com/en/article/4740366>

Download Persian Version:

<https://daneshyari.com/article/4740366>

[Daneshyari.com](https://daneshyari.com)